Environmental Pollution 243 (2018) 1791–1801

Contents lists available at ScienceDirect

Environmental Pollution

journal homepage: www.elsevier.com/locate/envpol

Ambient air quality in the holy city of Makkah: A source apportionment with elemental enrichment factors (EFs) and factor analysis (PMF)☆

Shedrack R. Nayebare [a, b], Omar S. Aburizaiza [c], Azhar Siddique [d], David O. Carpenter [a, e], Mirza M. Hussain [b], Jahan Zeb [c], Abdullah J. Aburiziza [f], Haider A. Khwaja [a, b, *]

[a] Department of Environmental Health Sciences, School of Public Health, University at Albany, State University of New York, Albany, NY, 12201, USA
[b] Wadsworth Center, New York State Department of Health, Albany, NY, 12201, USA
[c] Unit for Ain Zubaida Rehabilitation and Ground Water Research, King Abdulaziz University, Jeddah, Saudi Arabia
[d] Qatar Environment and Energy Research Institute, Hamad Bin Khalifa University, Qatar Foundation, Doha, Qatar
[e] Institute for the Health and the Environment, University at Albany, 5 University Place, Rensselaer, NY, 12144, USA
[f] School of Medicine, Umm Ul Qura University, Mecca, 21955, Saudi Arabia

ARTICLE INFO

Article history:
Received 19 April 2018
Received in revised form
17 September 2018
Accepted 17 September 2018
Available online 28 September 2018

Keywords:
$PM_{2.5}$
Black carbon
Trace elements
Enrichment factor
PMF
Makkah
Saudi Arabia

ABSTRACT

Air pollution remains a major global public health and environmental issue. We assessed the levels of $PM_{2.5}$ and delineated the major sources in Makkah, Saudi Arabia. Fine particulate matter ($PM_{2.5}$) sampling was performed from February 26, 2014–January 27, 2015 in four cycles/seasons. Samples were analyzed for black carbon (BC) and trace elements (TEs). $PM_{2.5}$ source apportionment was performed by computing enrichment factors (EFs) and positive matrix factorization (PMF). Backward-in time trajectories were used to assess the long-range transport. Significant seasonal variations in $PM_{2.5}$ were observed, Spring: 113 ± 67.1, Summer: 88.3 ± 36.4, Fall: 67.8 ± 24, and Winter: $67.6 \pm 36.9\ \mu g\ m^{-3}$. The 24-h $PM_{2.5}$ exceeded the WHO ($25\ \mu g\ m^{-3}$) and Saudi Arabia's ($35\ \mu g\ m^{-3}$) guidelines, with an air quality index (AQI) of "unhealthy to hazardous" to human health. Most delta–C computations were below zero, indicating minor contributions from bio-mass burning. TEs were primarily Si, Ca, Fe, Al, S, K and Mg, suggesting major contributions from soil (Si, Ca, Fe, Al, Mg), and industrial and vehicular emissions (S, Ca, Al, Fe, K). EF defined two broad categories of TEs as: anthropogenic (Cu, Zn, Eu, Cl, Pb, S, Br and Lu), and earth-crust derived (Al, Si, Na, Mg, Rb, K, Zr, Ti, Fe, Mn, Sr, Y, Cr, Ga, Ca, Ni and Ce). Notably, all the anthropogenic TEs can be linked to industrial and vehicular emissions. PMF analysis defined four major sources as: vehicular emissions, 30.1%; industrial-mixed dust, 28.9%; soil/earth-crust, 24.7%; and fossil-fuels/oil combustion, 16.3%. Plots of wind trajectories indicated wind direction and regional transport as major influences on air pollution levels in Makkah. In collusion, anthropogenic emissions contributed >75% of the observed air pollution in Makkah. Developing strategies for reducing anthropogenic emissions are paramount to controlling particulate air pollution in this region.

1. Introduction

Air pollution remains a critical problem in cities of developing nations, including Saudi Arabia and the rest of the Middle East. The Saudi economy is booming with significant industrialization, urbanization, and motor vehicle use. Thus, the number of both stationary (refineries, industries, etc.) and mobile (trucks, cars, buses, etc.) sources of air pollution have increased greatly. However, the implementation of regulations on emissions of particulate air pollutants is still insufficient, thus poor urban air quality continues to be an issue in Saudi Arabia's major cities (Nayebare et al., 2016; Alharbi et al., 2015; Al-Jeelani, 2009a). Saudi Arabia's climate is characteristically semi-arid to arid, as a result, air pollutants remain airborne longer. Though sand storms contribute a substantial proportion of air pollution in Saudi Arabia, several studies have shown a significant input from anthropogenic emissions mostly related to fossil-fuel combustion and vehicular emissions

☆ This paper has been recommended for acceptance by Dr. Jorg Rinklebe

* Corresponding author. Wadsworth Center, NYSDOH, Albany, NY, 12201, USA.
E-mail address: haider.khwaja@health.ny.gov (H.A. Khwaja).

https://doi.org/10.1016/j.envpol.2018.09.086
0269-7491/

(Nayebare et al., 2016; Alharbi et al., 2015; Munir et al., 2013; Khodeir et al., 2012; Nasrallah and Seroji, 2008). Thus, there is a need for more air quality assessments in Saudi Arabia's major urban areas.

The holy city of Makkah is unique. During the Holy Pilgrimage of Islam (Ramadhan and Hajj seasons), the city receives more than 4 million Muslim pilgrims from all over the world, every year (Al-Jeelani, 2009a; Al-Jeelani, 2009b; Nasrallah and Seroji, 2008). This means increased use of public transportation (buses, trucks, cars) to transport pilgrims and thus, increased consumption of gasoline and higher levels of dust resuspension. During the study period, Ramadhan was from June 29, 2014 to July 28, 2014 while Hajj week was from October 1–6, 2014. Air pollution emissions from vehicles can be significant. Indeed, previous studies have reported road traffic emissions from heavy trucks and buses, windblown dust/sand, gasoline evaporation, liquefied petroleum and air conditioners, as being the major sources of air pollution in Makkah (Simpson et al., 2014; Habeebullah, 2013; Al-Jeelani, 2009b). These studies reported elevated levels of several pollutants such as nitrogen dioxide (NO_2), carbon-monoxide (CO), sulfur dioxide (SO_2), ozone (O_3), methane (CH_4), volatile organic compounds (VOCs) and total hydrocarbons (HCs) especially during the Hajj. These air pollutants are primarily associated with vehicular emissions from heavy vehicles with some input from industrial processes (Nayebare et al., 2016).

Makkah city itself is not heavily industrialized; however, the neighboring cities of Jeddah, Rabigh and Yanbu are. The industrial emissions from these cities can be dispersed by wind into Makkah and all the surrounding areas. Makkah City is located 70 km southeast of Jeddah, 178 km southeast of Rabigh, and 351 km southeast of Yanbu. All three cities are Saudi Arabia's major industrial centers, and have several oil-fueled power plants, oil refineries, heavy petrochemical industries, large cement factories, desalination plants, mineral and metal industries, and several other small industries and workshops. Also, Makkah is about 1391 km southeast of Haifa's extensive industrial zone. This places Makkah City at possible crossroads of $PM_{2.5}$ convergence from different sources. Additionally, Makkah is a developing city, and had considerable ongoing construction work during the study period. Added to the heavy vehicle traffic, this significantly increased the air pollution levels.

In the current study, we provide a detailed assessment and delineation of various emission sources of fine particulate ($PM_{2.5}$) air pollution in the holy city of Makkah, based on the mass concentrations of $PM_{2.5}$ and its chemical constituents including black carbon (BC) and trace elements (TEs). Results from this study are crucial for informing the improvement and implementation of the existing policies on air pollution control in Makkah and the rest of Saudi Arabia.

2. Methods and materials

2.1. Study area

Makkah city is in the Makkah Province of Saudi Arabia (Fig. 1) at Latitude 21.4° N and Longitude 39.8° E, South of the Tropic of Cancer. The city is about 45 miles east of Jeddah, the Red Sea's major sea port, and is surrounded by the Sirat Mountains. Like the rest of Saudi Arabia, the temperatures are very warm to hot year-round. Winter temperatures are about 19 °C at night to approximately 29 °C in the afternoons, while summer temperatures are usually extremely hot (often exceeding 38 °C in the afternoons and dipping to about 32 °C in the evenings). Makkah receives very little rainfall, with an average annual total precipitation of 3.5 in (89.4 mm) that is mostly from September to January. Humidity is also highest during the same period and lowest (around 30%) from May to August (https://www.wunderground.com). Makkah has a permanent total population estimated at 1.3 million people (SADP, 2014) but the city is one of the busiest in Saudi Arabia especially during the holy months of Ramadan and Hajj as noted earlier.

2.2. $PM_{2.5}$ sampling and analysis

The 24-h $PM_{2.5}$ sampling was done from February 26, 2014 to January 27, 2015 at five sampling sites (Al-Haram, Rusaifa, Shokiya, Al-Hajj and Taneem) in Makkah City (Fig. 1). A blend of residential and urban/semi-industrial sampling sites was used for a balanced estimate of air pollution levels.

Al-Haram site represented the central area of Makkah. This area was central to all the religious activities. Presence of pilgrims and consequent transportation activities remained active day and night throughout the study period. The pilgrims' activities were highest during the months of Ramadan (fasting month) and Hajj (annual pilgrimage). This sampling site was also characterized by heavy construction work especially during cycles one and two (Spring and Summer seasons). *Rusaifa site* in Al-Rusaifa district, was located near to the intersection of Jeddah-Mecca highway and Al-Siteen Road. This area represented a combination of residential and commercial areas with local and pilgrims' activities. *Shokiya* site was in a residential area and represented emissions from the local permanent residences. *Al-Hajj site* (Shara-e-Hajj) was located at the intersection of Al-Hajj and Madina Roads. This was a commercial cum residential area characterized by busy local and pilgrims' activities. *Taneem site* was located near Al-Noor Hospital in the Tanseem district and it represented mainly the pilgrimage movement with some commercial activities. This sampling site was at the entrance of Makkah City, about 8 Km from the central area.

Sampling was done for approximately 7 weeks (50 days) in cycle_1 (Spring), 9 weeks (61 days) in cycle _2 (Summer), and 6 weeks (42–44 days) in cycles_3 (Fall) and 4 (Winter). Cycle_1 was from February 26, 2104 to April 16, 2014 at Al-Haram and Rusaifa; cycle_2 from June 5, 2014 to August 4, 2014 at Al-Haram, Shokiya and Al-Hajj; cycle_3 from September 16, 2014 to October 29, 2014 at Al-Haram, Shokiya and Al-Hajj; and cycle_4 from December 15, 2014 to January 27, 2015 at Al-Haram and Taneem. Th extended sampling during Spring and Summer seasons was intended to monitor pollution levels during the days with pilgrim activities (Ramadan and Hajj seasons). We missed a few days of sampling during Fall and Winter seasons due to electricity outages. Together, the 4 cycles make up the study period, with each cycle representing one season of the year. The average of the 24-h $PM_{2.5}$ levels from various sampling sites was used as the overall 24-h $PM_{2.5}$. This was thought to be a more representative estimate of the daily ambient $PM_{2.5}$ and its chemical components. More details of the $PM_{2.5}$ sample preparation, collection, processing (storage, conditioning, inspection, weighing), and analysis for $PM_{2.5}$ mass concentrations, have been provided previously (Nayebare et al., 2016; Nayebare, 2016).

We performed a $PM_{2.5}$ mass-reconstruction (data not presented) using the analyzed pollutant species (BC and TEs), as shown in our previous work (Nayebare et al., 2016). The following were the proportions of explained variation in $PM_{2.5}$ by cycle (season): cycle_1 (Spring), 64.3%; cycle_2 (Summer), 59.3%; cycle_3 (Fall), 40.4% and cycle_4 (Winter), 44.8%. The unexplained variation can be attributed to other pollutant species such as the water-soluble ionic species, particulate organic carbon, PAHs, and secondary aerosols, not analyzed in this study. The source apportionment and any derived conclusions in this study were based only on the explained proportion of the observed $PM_{2.5}$.

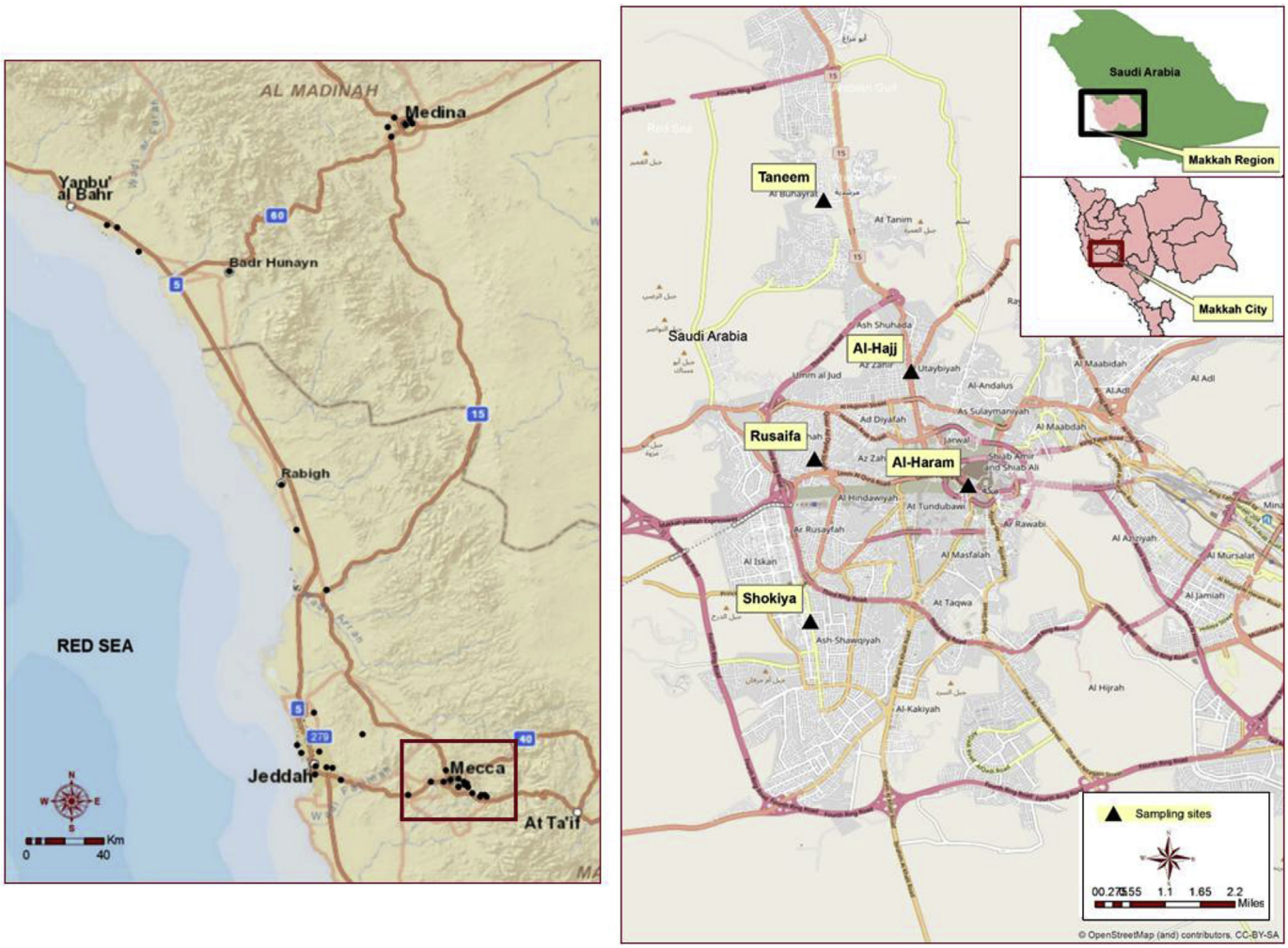

Fig. 1. Map of Makkah showing the $PM_{2.5}$ sampling sites (Al-Haram, Rusaifa, Shokiya, Al-Hajj and Taneem).

2.3. Analysis of black carbon (BC)

BC was analyzed from $PM_{2.5}$ filters by dual-wavelength Optical Transmissometer [Model OT-21, 2007], as previously described by Nayebare et al. (2016). BC concentration ($\mu g\ m^{-3}$) at ultraviolet (UV, $\lambda = 370$ nm) and infrared (IR, $\lambda = 880$ nm) wavelengths, was calculated based on sampled air volume (m^3) and exposed filter area (16.8 cm^2). BC at $\lambda = 880$ nm, represents the actual BC (soot), while BC at $\lambda = 370$ nm represents the non-black components of BC such as PAHs. Attenuation coefficients $K_{880\ nm} = 16.6\ m^2\ g^{-1}$ and $K_{370\ nm} = 39.5\ m^2\ g^{-1}$ (Ahmed et al., 2009) were applied at respective channels to correct for filter loading effects. The difference between $BC_{370\ nm}$ and $BC_{880\ nm}$ estimates delta−C (Eq. (1)), a good marker for organic matter combustion (Rattigan et al., 2013; Wang et al., 2012).

$$\mathbf{Delta{-}C} = \mathbf{BC}_{\lambda=370\ nm} - \mathbf{BC}_{\lambda=880\ nm} \quad (1)$$

2.4. Analysis of TEs

TEs in $PM_{2.5}$ samples were analyzed by an ARL QUANT'X Energy Dispersive X-ray Fluorescence (ED−XRF) spectrometer (model AN41903−E 06/07C, Ecublens Switzerland). The instrument was energy (eV) calibrated for every sample sequence. As a quality control (QC) measure, a QC sample was analyzed before and after every sequence, and sample holders thoroughly cleaned with deionized water and a micro® liquid soap per sequence to prevent cross contamination. ED−XRF has been applied in several studies for TEs analysis in PM samples (Shaltout et al., 2013; Yatkin et al., 2012; Xu et al., 2012), because it is fast and does not require chemical digestion of samples prior to analysis (Korzhova et al., 2011). This greatly minimizes sample contamination.

The technique works on a principle that, distinct atoms in a sample, emit x-ray photons with characteristic energy and wavelength when excited by an external high energy. Thus, by measuring the intensity of photons per emitted energy, TEs in a sample are identified and quantified (Margui and Van Grieken, 2013; Buhrke et al., 1998). Typically, the intensity of radiation signal from each TE in the sample, is proportional to its concentration. TE concentrations are computed from a set of internal calibration curves and displayed in ng cm^{-2}, which we then converted to ng m^{-3} based on the exposed filter area and sampled air volume.

ED−XRF technique can perform multi-elemental analysis (Na to U in concentration range of 100% down to sub-ppm level) while simultaneously providing concentration and uncertainty data, with high precision and reliability. Major limitations relate to low sensitivity for lighter TEs ($z < 11$) due to their inherent low

fluorescent yield (Margui and Van Grieken, 2013); and absorption of low energy x-rays by the filter material and particle deposits (Ozturk et al., 2011). In the current study, membrane filters with surface deposition were used and thus minimizing x-ray absorption by the filter material. We verified the validity of TEs data by comparing the concentration and uncertainty of each TE. Only those TEs with concentrations above the detection limit (DL) and at least 3 times the uncertainty, were reported in this study. The typical DLs of TEs were reported in our previous work (Nayebare et al., 2016).

2.5. Source apportionment

The delineation of $PM_{2.5}$ sources was done using computations of elemental enrichment factors (EFs), and a factor analysis/positive matrix factorization (PMF). Additionally, plots of 72-h backward-in-time wind trajectories were used to assess any possible contributions from long-distance transport of $PM_{2.5}$ aerosols.

2.5.1. Enrichment factors (EFs)

The extent of anthropogenic contribution of TEs was calculated based on their degree of enrichment in $PM_{2.5}$ compared to the earth-crust (Reimann and Caritat, 2000) as shown in *Eq.* (2). EFs have been used in several studies to study the sources of air pollution (Fabretti et al., 2009; Aprile and Bouvy, 2008). Aluminum was used as reference element due to its high relative abundancies in the earth-crust.

$$\mathbf{EF} = \frac{(\mathbf{C_X}/\mathbf{C_{Al}})_{\mathbf{PM_{2.5}}}}{(\mathbf{C_X}/\mathbf{C_{Al}})_{\mathbf{earth\ crust}}} \quad (2)$$

where, $\mathbf{C_X}$ = concentration of trace metal/element X; and $\mathbf{C_{Al}}$ = concentration of Al.

We used TEs relative abundances in the earth-crust reported by Taylor (1964). An EF of 10 was used as a baseline to account for any background levels. EF $\leq$ 10 indicates significant contributions from earth-crust, while EF > 10 is indicative of significant anthropogenic contributions (Kłos et al., 2011). EFs provide a meaningful source apportionment, especially when used in conjunction with other analyses such as PMF.

2.5.2. Positive matrix factorization (PMF)

We applied PMF (version 5.0.14) to delineate the various sources of $PM_{2.5}$ in Makkah. There we some variations in pollutant species per cycle, reflecting seasonal variations as shown in Table 1. The relative source contributions presented in this study were based on the data from combined cycles/seasons. However, the emission sources of PM vary significantly by season. Thus, we performed additional PMF analyses by cycle (season) to assess any seasonal variations in sources of particulate air pollution. The results for individual cycles are presented in the supplemental materials (Tables S_5 to S_6 and Figures S_3 to S_6). Only the results from PMF model with combined cycles, are emphasized throughout this study. Following several analytical runs, the PMF base models for both combined and individual cycles were finally set at 20 runs with four factors. Each model was run more than five times to ensure consistency in the obtained results (as a QA/QC measure). Given the right number of factors, the base model results are consistent following multiple analyses and attain 100% convergence for all the analytical runs. We used this criterion to select the number of factors used in the base models.

The observed Q-robust and Q-true values remained constant and were within the same range following multiple model runs. Additionally, the models attained a 100% convergence rate for all the analytical runs. This confirmed the accuracy of the number of factors used for analysis. Though all the Q-values were close to each other (Table S_3), the model by default selects and displays results for the run with the lowest Q-robust value. The PMF results based on model run number 10 are highlighted in Table S_3. No major differences between the runs were found. The Q-robust values are based on the model with controlled outliers, while the Q-true values are for a model that includes the outliers. Thus, the observed slight differences between the two Q-values imply that the models attained a good fit for the data and the outliers.

Residual analyses indicated that most of the pollutant species had normally distributed residuals and relatively high signal-to-noise ratios (S/N) except for V, Ga, Zr, Ce, Pr, Eu and Er (Table S_4), all of which had S/N < 5.0 and were all classified as “weak” to limit their influence on the model results. These pollutants (TEs) were mostly below their detection limits in $PM_{2.5}$ for a major part of the study period. Also, $PM_{2.5}$ as an input parameter, was restricted from strongly influencing the model results since we delineated the sources of $PM_{2.5}$ in this analysis. All the species with S/N > 5 were classified as “strong” in the PMF base model. Additional summaries of the S/N, pollutant categories, and residual distributions of the pollutants used for PMF analysis are presented in Table S_4. More discussions of PMF analysis, resolution and data interpretation for source identification can be found in the literature (Fabretti et al., 2009; Sofowote et al., 2008; Hopke, 2000).

3. Results and discussion

3.1. $PM_{2.5}$ mass and chemical composition

The average 24-h $PM_{2.5}$, its chemical constituents (BC and TEs), and meteorology indicators including temperature, relative humidity (RH), and wind speed (WS) during the study are shown in Table 1. The 24-h $PM_{2.5}$ levels showed significant temporal variability, and far exceeded the WHO guideline (25.0 $\mu g\,m^{-3}$). More than 99.9% of the study period had daily $PM_{2.5}$ levels that exceeded this guideline (Table 1 and Fig. 2). Average levels during cycle_1 were 113 ± 67.1 (31–372); cycle_2, 88.3 ± 36.4 (40.1–262); cycle_3, 67.8 ± 24 (24–151); and cycle_4, 67.6 ± 36.9 (27.9–196) $\mu g\,m^{-3}$. As shown in Fig. 2, the $PM_{2.5}$ levels were lowest from September to January. Given that Makkah's climate is predominantly dry for most part of the year, the little rain fall received during the months of November to January (http://us.worldweatheronline.com/mecca-weather-averages/makkah/sa.aspx) may play little to no role in moderating air pollution levels. The variations in the atmospheric boundary layer across different seasons may have a major influence in the observed $PM_{2.5}$ levels. Thus, the observed high levels of air pollution during Spring and Summer seasons may be linked to a lower atmospheric boundary layer and thus reduced dispersion of air pollutants. $PM_{2.5}$ levels also spiked up to more than 260 $\mu g\,m^{-3}$ during the holy month of Ramadhan (June 29, 2014 to July 28, 2014) and the Hajj week (October 1–6, 2014) up to 140 $\mu g\,m^{-3}$, indicating an increase in heavy automobile use for transportation and the associated dust resuspension.

Similarly, BC at both IR and UV wavelengths displayed significant temporal variability (Fig. 2). Average BC_{IR} and BC_{UV} per cycle were 3.1 ± 1.0 and 2.6 ± 0.8 $\mu g\,m^{-3}$ in cycle_1, 1.8 ± 0.8 and 1.6 ± 0.6 in cycle_2, 1.6 ± 0.7 and 1.4 ± 0.5 in cycle_3 and 2.2 ± 0.9 and 1.6 ± 0.6 $\mu g\,m^{-3}$ in cycle_4 (Table 1). These relatively elevated levels of BC are indicative of significant contribution from local vehicular emissions and long-distance transport. There were no clear distinct trends for weekend/weekday variations in either $PM_{2.5}$ or BC. Overall BC, as represented by a signal at BC_{IR}, explained 2.6%, 2.1%, 2.4%, and 3.6% of the total variation in $PM_{2.5}$ during cycles 1 to 4, respectively. The average delta–C estimates per cycle, as computed from the difference of BC_{UV} and BC_{IR} (Nayebare et al., 2016), were in

Table 1
Summary of the overall levels of 24-h $PM_{2.5}$, black carbon (BC), trace elements (TEs), and meteorology (temperature, relative humidity – RH and wind speed – WS) during the study in Makkah, Saudi Arabia.

Component	Cycle_1 (Spring): 2014-2			Cycle_2 (Summer): 2014-3			Cycle_3 (Fall): 2014-4			Cycle_4 (Winter): 2015-1			DR (%)
	Mean ± S.D	Min	Max	Mean ± S.D	Min	Max	Mean ± S.D	Min	Max	Mean ± S.D	Min	Max	
$PM_{2.5}$ ($\mu g\ m^{-3}$)	113 ± 67.1	31	372	88.3 ± 36.4	40.1	262	67.8 ± 24	24	151	67.6 ± 36.9	27.9	196	NA
BC_{IR} ($\mu g\ m^{-3}$)	3.1 ± 1.0	1.2	5.2	1.8 ± 0.8	0.5	4.1	1.6 ± 0.7	0.6	3.6	2.2 ± 0.9	1.0	5.1	100
BC_{UV} ($\mu g\ m^{-3}$)	2.6 ± 0.8	1.1	4.6	1.6 ± 0.6	0.5	3.4	1.4 ± 0.5	0.5	2.8	1.6 ± 0.6	0.8	4.1	100
Delta-C ($\mu g\ m^{-3}$)	−0.5 ± 0.2	−0.9	0.1	−0.2 ± 0.3	−0.8	0.6	−0.2 ± 0.2	−0.9	0.1	−0.6 ± 0.3	−1.4	0.1	NA
RH (%)	45 ± 6.9	31	58	30.2 ± 6.8	21	51	46.7 ± 7.9	30	62	59.6 ± 9.9	34	74	NA
Temperature (°F)	30.2 ± 2.45	23.3	34.4	37.3 ± 1.46	34.4	41.1	34.5 ± 1.58	31.1	37.8	26.1 ± 2.47	20.0	30.0	NA
Wind Speed ($m\ s^{-1}$)	6.5 ± 4.2	2.0	22	5.0 ± 2.3	2.0	14	5.6 ± 2.6	2.0	17	4.5 ± 2.1	2.0	9.0	NA
Trace Elements ($ng\ m^{-3}$)													
Silicon (Si)	14235 ± 7863	3362	36296	10143 ± 4489	3138	30380	4869 ± 3036	1160	13883	5559 ± 4350	1861	23661	100
Calcium (Ca)	10707 ± 6792	2167	27102	7441 ± 3539	2114	17194	3625 ± 3120	1027	15407	4535 ± 3595	1153	19209	100
Iron (Fe)	6712 ± 4867	1382	26652	5334 ± 2953	1726	21621	2302 ± 1557	531	8366	2536 ± 1938	823	10420	100
Aluminum (Al)	4826 ± 2678	1072	12418	3698 ± 1677	1323	11323	2735 ± 1229	1019	7276	2212 ± 1560	676	8429	100
Sulfur (S)	4624 ± 1635	1629	8481	3273 ± 1697	1217	9450	5533 ± 1818	2801	10920	3915 ± 1684	1628	9546	100
Potassium (K)	1525 ± 930	423	4865	1056 ± 405	446	2692	614 ± 324	301	1708	679 ± 420	256	2342	100
Magnesium (Mg)	1475 ± 833	408	3962	946 ± 389	310	2361	507 ± 309	168	1336	580 ± 439	168	2670	100
Sodium (Na)	1018 ± 243	583	1470	706 ± 267	295	1383	881 ± 369	308	1887	681 ± 209	345	1231	100
Chlorine (Cl)	644 ± 492	<1.68	1962	685 ± 382	<1.68	1541	492 ± 643	<1.68	2087	488 ± 487	<1.68	1742	81.9
Titanium (Ti)	569 ± 387	122.1	2078	453 ± 256	142	1875	198 ± 142	43.0	736	241 ± 184	78.0	921	100
Manganese (Mn)	145 ± 102	32.4	563.3	112 ± 58.1	35.9	406	50.6 ± 30.4	20.7	160	54.5 ± 36.8	19.3	205	100
Zinc (Zn)	105 ± 41.9	38.9	261.4	81.4 ± 42.8	27.3	268	53.9 ± 23.6	21.0	117	58.9 ± 30.7	21.8	152	100
Lead (Pb)	82.7 ± 115	1.38	743.2	97.7 ± 258	4.70	1290	65.3 ± 60.2	6.10	245	26.1 ± 45.5	<1.09	239	99.5
Bromine (Br)	73.5 ± 24.6	41.7	168.3	61.2 ± 17.6	20.1	105	63.4 ± 17.9	28.5	102	57.6 ± 23.7	34.0	136	100
Strontium (Sr)	65.6 ± 45.8	12.1	206.9	44.7 ± 21.9	12.2	120	21.7 ± 17.5	5.30	93.0	24.4 ± 18.1	8.00	98.0	100
Erbium (Er)	50.3 ± 27.2	14.7	129.8	39.4 ± 18.3	12.2	109	20.0 ± 11.5	5.90	60.3	22.3 ± 14.9	6.20	78.0	100
Lutetium (Lu)	43.2 ± 21.2	14.7	103.9	34.8 ± 15.6	13.7	92.3	20.8 ± 9.55	6.60	52.7	21.2 ± 11.5	8.90	65.8	100
Copper (Cu)	30.5 ± 15.4	9.71	68.0	32.4 ± 12.4	15.4	76.3	26.4 ± 10.9	9.80	56.0	18.0 ± 11.4	5.10	52.7	100
Nickel (Ni)	23.6 ± 13.6	7.22	75.0	18.9 ± 8.32	7.78	54.9	12.6 ± 5.56	4.85	29.2	11.1 ± 5.56	3.94	34.3	100
Cerium (Ce)	21.5 ± 12.4	<1.98	57.0	21.3 ± 9.13	8.17	57.6	12.5 ± 9.19	<1.98	38.8	11.6 ± 9.23	<1.98	43.3	95.0
Chromium (Cr)	21.4 ± 14.6	4.62	78.3	18.0 ± 8.83	5.70	59.0	11.0 ± 5.76	4.34	36.0	9.82 ± 6.41	3.21	35.7	100
Zirconium (Zr)	17.0 ± 17.9	<1.09	68.7	22.4 ± 13.3	<1.09	56.1	–	–	–	–	–	–	41.2
Praseodymium (Pr)	16.5 ± 10.7	<1.98	53.0	16.3 ± 7.89	<1.98	51.8	8.87 ± 7.52	<1.98	25.4	7.39 ± 5.20	<1.98	24.3	89.4
Rubidium (Rb)	7.06 ± 5.68	<0.59	32.3	5.80 ± 2.46	2.81	18.0	2.31 ± 2.12	<0.59	9.1	3.02 ± 2.36	<0.59	12.5	87.4
Yttrium (Y)	5.79 ± 4.96	<0.98	29.5	6.13 ± 8.44	<0.98	44.0	3.31 ± 2.25	<0.98	10.0	4.19 ± 2.42	<0.98	10.3	84.9
Gallium (Ga)	3.55 ± 3.73	<0.59	18.7	4.06 ± 2.97	<0.59	13.6	–	–	–	–	–	–	38.2
Vanadium (V)	–	–	–	7.08 ± 10.5	<0.98	43.8	14.1 ± 8.17	<0.98	31.0	5.22 ± 7.03	<0.98	21.4	38.7
Europium (Eu)	–	–	–	5.60 ± 7.06	<1.98	27.1	–	–	–	–	–	–	11.1

Cycle_1 (Spring): Feb 26th – Apr 16th, 2014 (Al-Haram & Rusaifa), **Cycle_2 (Summer):** Jun 5th – Aug 4th, 2014 (Al– Haram, Shokiya & Al-Hajj), **Cycle_3 (Fall):** Sep 16th – Oct 29th, 2014 (Al-Haram, Shokiya & Al-Hajj), **Cycle_4 (Winter):** Dec 15th, 2014–Jan 27th, 2015 (Al-Haram & Taneem). **DR (%):** Overall detection rate of various pollutants measured from $PM_{2.5}$.

negative values as shown in Table 1. Positive delta–C estimates are indicative of bio-mass combustion as a source of $PM_{2.5}$ (Rattigan et al., 2013; Wang et al., 2012; Wang et al., 2011). Thus, combustion of bio-mass was not a major $PM_{2.5}$ emission source in Makkah.

Also, comparing the $PM_{2.5}$ levels by site and season indicated a consistently higher pollution levels at Al-Haram sampling site compared to any other site (Fig. 3A). The high levels of $PM_{2.5}$ at Al-Haram sampling site during cycle_1 (Spring) were mostly attributed to heavy construction work while during cycle_2 (Summer), the high $PM_{2.5}$ levels coincided with Ramadhan period (June to August). Similarly, the BC levels were highest at Al-Haram as shown in Fig. 3B. This highlighted the major anthropogenic contribution related to vehicular and construction works, to the overall pollution levels in Makkah city. Additionally, the observed pollution levels exceeded the Saudi Arabia's presidency for meteorology, PME ($35\ \mu g\ m^{-3}$) and WHO ($35\ \mu g\ m^{-3}$) guidelines, even at residential sampling sites, further underscoring the poor air quality in Makkah City.

More than 25 trace elements (TEs) were detected from $PM_{2.5}$ samples (Table 1). TEs, including Si, Ca, Fe, Al, K, Mg, and Na, consistently had the highest concentrations suggesting a significant contribution from the soil to the observed $PM_{2.5}$. The elevated levels of sulfur (S) are indicative of industrial emissions occurring locally as well as those due to long-distance transport from the neighboring cities of Jeddah and Rabigh, as shown by the wind trajectories (Figures S_8 to S_{11}). Also, a portion of Na and Cl levels may be attributed to long-range transport of marine aerosols from the Red Sea. Makkah is only 45 km west of the Red Sea, making the transport of sea-salt by wind possible as shown by the backward-in-time wind trajectories in Figures S_8 to S_{11}.

Several anthropogenic TEs, including Pb, Lu, Br, V, Cu, Ti, Zn, Ni, Sr, Ce, Er, and Cr were also detected in $PM_{2.5}$ samples (Table 1). These TEs are primarily due to the vehicular emissions (Pb, Ni, Cu, Br, Sr, Zn, Ti, Ce), fossil fuels combustion (V, Lu, Er, Pb), and other industrial processes (Nayebare et al., 2016).

3.2. Air quality index (AQI)

AQI was computed based on the average daily $PM_{2.5}$ levels. During most days of the study period we recorded an AQI rated on the scale of unhealthy to hazardous. There were no days with good air quality. At Al-Haram (cycle_1) 39.3% (20 days) had an unhealthy AQI; 36.7% (18 days) had a very unhealthy AQI, 17.9% (9 days) had hazardous air quality; and 6.1% (3 days) had AQI levels that were unhealthy for sensitive sub-groups (Figure S_1). The poor air quality in Makkah is attributable to several factors. Notably, much ongoing construction works occurred during the study period, which greatly increased dust resuspension, resulting in elevated $PM_{2.5}$ levels. Additionally, other $PM_{2.5}$ sources, such as local vehicular and regional industrial emissions, also contributed significantly to the

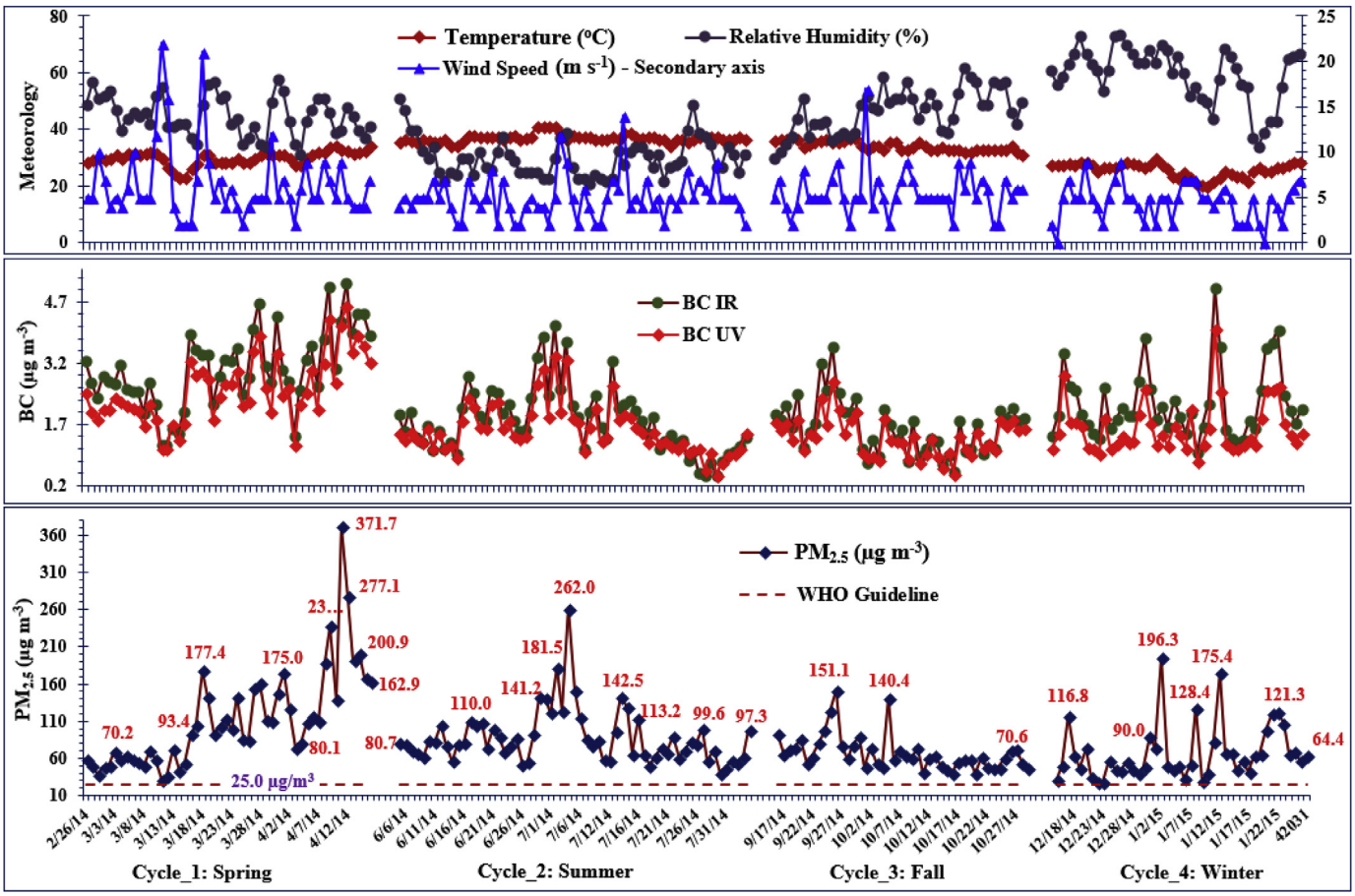

Fig. 2. Time-series plots of the average 24-h $PM_{2.5}$, BC and Meteorology during the study in Makkah, Saudi Arabia.

ambient $PM_{2.5}$. Overall, the computed AQI indicates that air pollution in Makkah is a major issue. $PM_{2.5}$ emissions, particularly from automobiles and industries, are common to developing countries worldwide. Our observations emphasize the need for improved control measures to reduce human exposure.

The $PM_{2.5}$ levels recorded in Makkah were markedly higher than $PM_{2.5}$ levels reported for most cities in developed countries (Fig. 4). Only the Asian cities in China, Bangladesh, Mongolia, and India had $PM_{2.5}$ levels comparable with levels measured in Makkah. Also, the observed $PM_{2.5}$ levels exceeded the WHO (25 µg m^{-3}) and the Saudi Arabia Presidency of Meteorology and Environment (PME) (35 µg m^{-3}) guidelines for 24-h $PM_{2.5}$. This finding is likely to reflect the inadequate application of the existing policies. Thus, strategies for improving the implementation of the existing PME regulation are needed.

3.3. Pearson correlations between pollutant species and with meteorology

Intercorrelations between $PM_{2.5}$, its constituents (BC, TEs), and meteorology indicators are summarized in Table S_1. $PM_{2.5}$ was weakly correlated with temperature ($r = 0.17$, p-value <.0001) and RH ($r = -0.21$, p-value .0038), but was not correlated with wind speed. The mean daily temperature showed a very slight seasonal variability (Table 1) but no significant daily variability over the entire study period (Fig. 2). However, relative humidity (RH) showed a significant temporal variability as shown in Table 1 and Fig. 2. One would expect that an increase in RH to strengthens the hygroscopic growth of ambient PM, leading to an increase in PM levels. The observed inverse correlation between $PM_{2.5}$ and RH may be linked to the high ambient temperatures. Elevated ambient temperatures can lead to unstable atmospheric conditions characterized by intense convective air currents. Thus, any increase in RH may not significantly influence $PM_{2.5}$ levels due to rapid dispersion.

$PM_{2.5}$ was strongly correlated ($r \geq 0.90$, p-value <.0001) with crustal elements (Mg, Al, Si, K, Ca, Ti, Cr, Mn, Fe, Ni, Sr, Rb, Pr, Ce, Zr and Ga), suggesting a significant contribution from the soil/earth-crust. The semi-arid to arid climatic conditions, plus the heavy construction work during the study significantly contributed to elevated $PM_{2.5}$ levels. $PM_{2.5}$ also had moderate to high correlations with some anthropogenic TEs; Er ($r = 0.90$), Lu ($r = 0.90$), Cu ($r = 0.79$), Zn ($r = 0.66$), Br ($r = 0.46$), p-value <.0001 and weak correlations with Pb ($r = 0.18$, p-value = .01) and S ($r = 0.15$, p-value = .03). These TEs are primarily associated with vehicular and industrial emissions from fossil-fuels/oil combustion (Nayebare et al., 2016), which further highlights the contribution of vehicles and industries to the overall air pollution in Makkah, Saudi Arabia.

$PM_{2.5}$ was also moderately correlated (p-value <.0001) with Cl ($r = 0.39$) and Na ($r = 0.33$), suggesting some contributions from marine aerosols. Cl was moderately correlated with Na ($r = 0.52$), Ca ($r = 0.51$), K ($r = 0.47$) and Mg ($r = 0.46$), p-value <.0001. These TEs are components of sea-salt. Long-distance transport of marine aerosols from the Red Sea may be a significant source, as shown by the plots of backward-in-time trajectories (Figures $S_8 - S_{11}$).

Sulfur (S) was moderately correlated with V ($r = 0.54$), Pb ($r = 0.39$) and BC ($r = 0.29$), p-value <.0001, suggesting some contribution from industrial emissions. Long-distance transport of

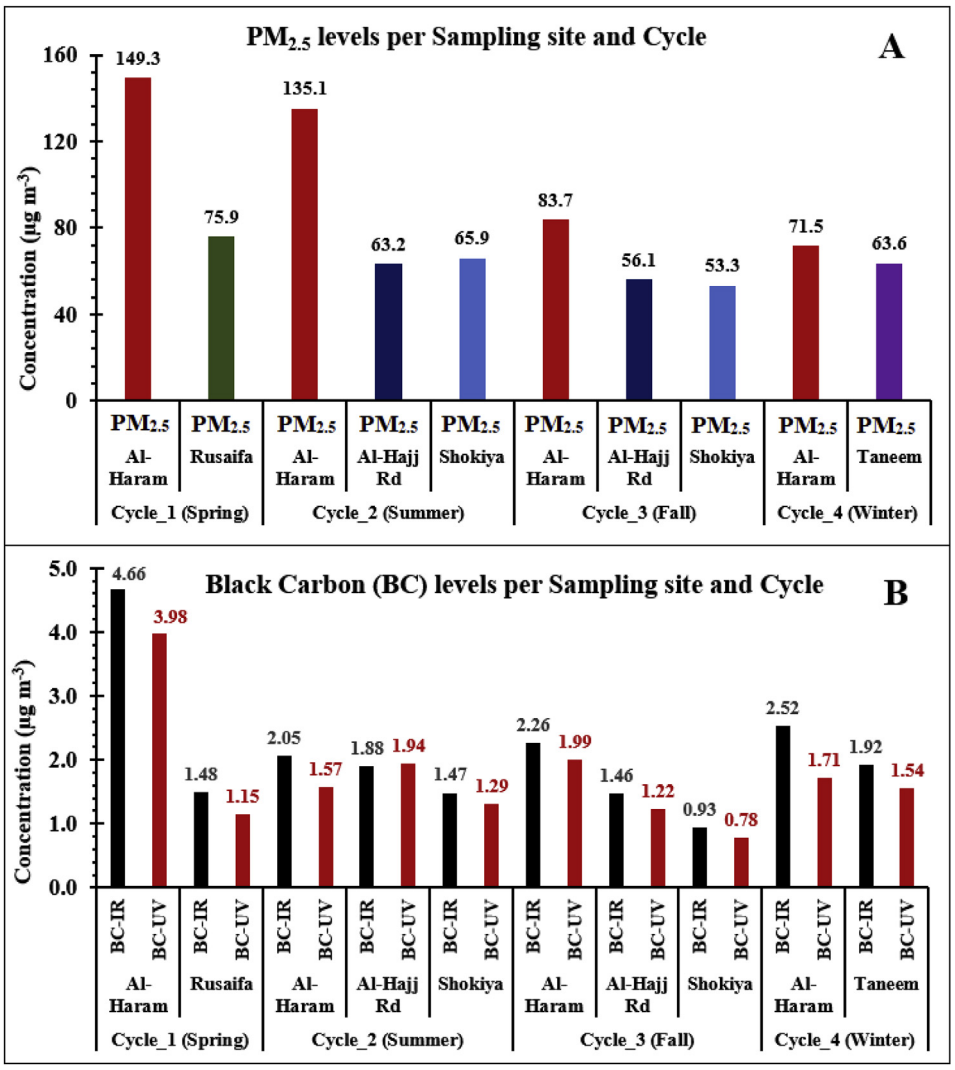

Fig. 3. Bar graphs showing the average $PM_{2.5}$ and BC levels by sampling site and cycle (season).

industrial emissions, as shown by the backward-in-time wind trajectories, may be a major influence on air pollution in Makkah.

BC was strongly correlated with $PM_{2.5}$ ($r = 0.70$), Ni ($r = 0.71$), Cu ($r = 0.60$), Zn ($r = 0.77$), Br ($r = 0.58$), Sr ($r = 0.72$), Ce ($r = 0.57$), Er ($r = 0.77$), and Lu ($r = 0.78$), p-value <.0001, indicating major contributions from the key sources of BC (vehicular and industrial emissions).

3.4. Sources of $PM_{2.5}$ — elemental enrichment factor (EF) analysis

TEs in $PM_{2.5}$ are of both natural and anthropogenic origins. We broadly defined these two sources using EF values as shown in Fig. 5 and supplemental materials (Table S_2 and Figure S_2). Anthropogenic TEs were defined with EF values greater than 10 while the earth-crust derived TEs, had EFs less than 10 (Nayebare et al., 2016). Though classified as anthropogenic, high Cl levels are typically indicative of marine input. Al, Si, Na, Mg, Rb, K, Zr, Ti, Fe, Mn, Sr, Y, Cr, and Ca had EFs <5 (Table S_2), suggesting a major input from the earth-crust. Most of these elements are naturally highly enriched in the soil. The classification of any TE as earth-crust derived simply implies that a major proportion of the given TE in air was enriched from the soil. Thus, there is a possibility of anthropogenic contribution, but in minor proportions. This can be further clarified by factor analysis with PMF to show all the contributing sources, as discussed in Section 3.5.

Cu, Zn, Eu, Pb, S, Br, and Lu consistently had EF values above 10, suggesting significant contributions from anthropogenic activities. Emissions of S are usually associated with fossil-fuels/oil combustion. In addition to local emissions, long-distance transport of industrial emissions from the neighboring industrialized cities of Jeddah and Rabigh may have contributed significantly to S levels in Makkah. Cu, Zn, Br and Pb may originate from both industrial and vehicular emissions. Leaded gasoline was phased-out more than a decade ago, but Pb is still ubiquitous in the environment as seen in this study. Br was also used in leaded gasoline as an essential component of “engine anti-knock fluid”. The phase-out of leaded gasoline implies a decline in the use of Br for this purpose. However, Br compounds are currently used in batteries of electric storage devices, electric cars designed to produce zero air pollution emissions, and several other applications (water treatment, pesticides, drugs). This explains the continued high levels of Br in the environment seen in this study.

Rare-earth elements (Ce, Lu, Er, Y) were also detected in $PM_{2.5}$. Detectable levels of these TEs in $PM_{2.5}$ may be indicative of anthropogenic applications. The stable Lutetium isotopes (^{175}Lu, ^{176}Lu) are used primarily as catalysts in the petroleum industry for

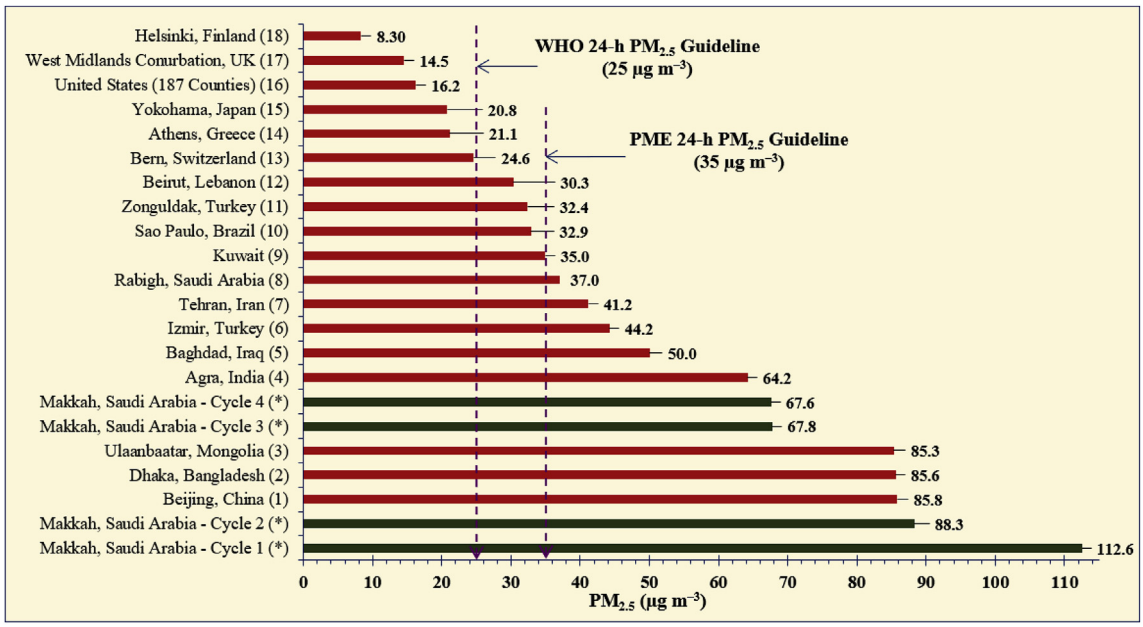

1 – (Zhao et al., 2009); 2 – (Begum et al., 2012); 3 – (Amarsaikhan et al., 2014); 4 – (Kulshrestha et al., 2009); 5 – (Hamad et al., 2015); 6 – (Yatkin and Bayram, 2008); 7 – (Kermani et al., 2015); 8 – (Nayebare et al., 2016); 9 – (Brown et al., 2008); 10 – (Degobbi et al., 2011); 11 – (Akyuz and Cabuk, 2009); 12 – (Nakhle et al., 2015); 13 – (Hueglin et al., 2005); 14 – (Pateraki et al., 2013); 15 – (Khan et al., 2010); 16 – (Bell et al., 2007); 17 – (Anderson et al., 2001); 18 – (Sillanpää et al., 2005); ***Makkah Cycles (1 – 4) – this study

Fig. 4. A bar graph showing the comparison of 24-h $PM_{2.5}$ levels measured in Makkah and other cities worldwide, and with the WHO and the Saudi Arabia's Presidency of Meteorology and Environment (PME) guidelines (Akyuz and Cabuk, 2009; Amarsaikhan et al., 2014; Anderson et al., 2001; Begum et al., 2012; Bell et al., 2007; Brown et al., 2008; Degobbi et al., 2011; Hamad et al., 2015; Hueglin et al., 2005; Kermani et al., 2015; Khan et al., 2010; Kulshrestha et al., 2009; Nakhle et al., 2015; Pateraki et al., 2013; Sillanpää et al., 2005; Yatkin and Bayram, 2008; Zhao et al., 2009).

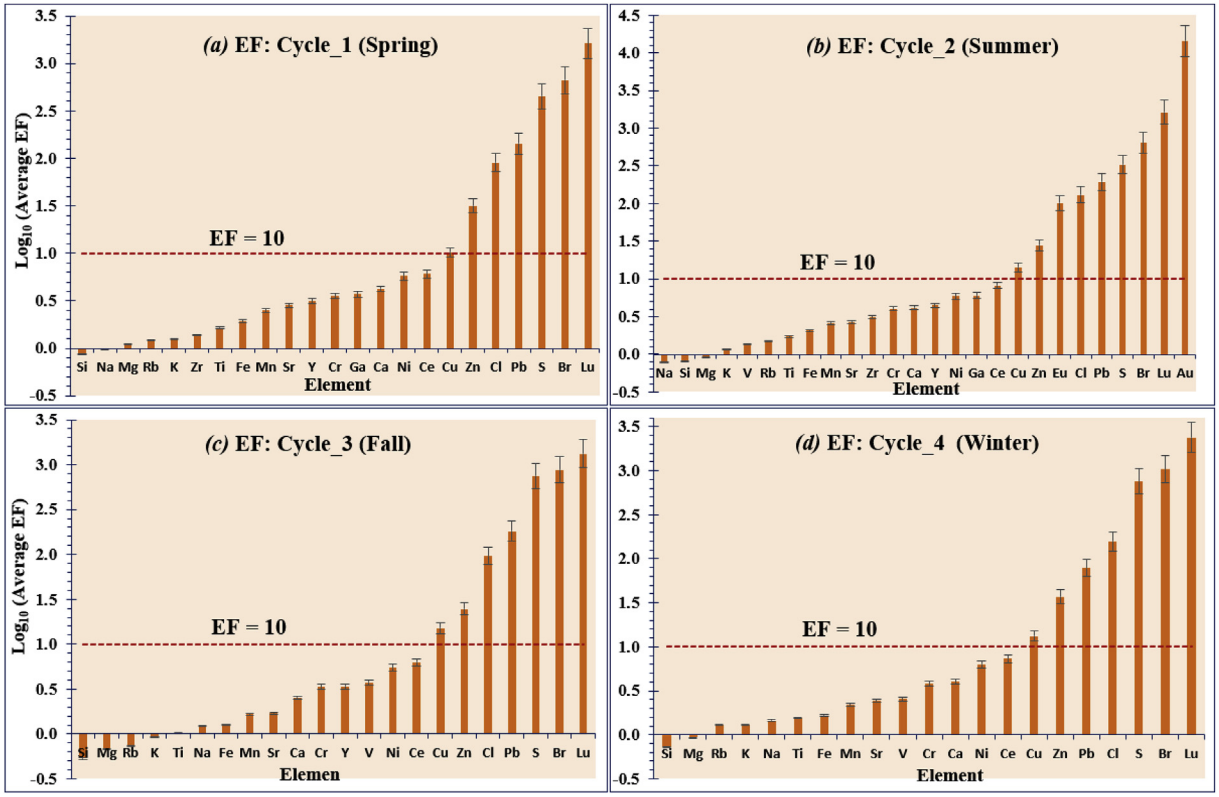

Fig. 5. Graphs *(a–d)* show the log transformed enrichment factors (EFs) for the trace elements (TEs) measured from $PM_{2.5}$ per cycle – averaged sampling sites.

cracking hydrocarbons in oil refineries, alkylation, hydrogenation and polymerization processes (RSC, 2016; Nayebare et al., 2016). Thus, Lu in air may be due to petrochemical-related industrial emissions.

Though classified as earth-crust derived in this study, the oxides of Ce have several commercial applications such as catalysts or additives to fuel to reduce emissions from automobiles (Bleiwas, 2013; Zeng et al., 2012). Cerium (II) oxide (CeO) is used as a hydrocarbon catalyst in self-cleaning ovens (Zeng et al., 2012) and petroleum cracking (Steinbach, 2011; Trovarelli, 2002), while cerium (III) oxide (Ce_2O_3) is used as a catalytic converter for the oxidation of CO and NO_X emissions from automobiles (Bleiwas, 2013), and cerium (IV) oxide (CeO_2) is used in glass polishing powders and phosphors in screens and fluorescent lamps. Thus, a sizable portion of Ce in air may originate from industrial and vehicular emissions.

3.5. *Sources of $PM_{2.5}$ — positive matrix factorization (PMF) analysis*

The relative source contributions are presented in Fig. 6 and in supplemental materials (Tables $S_3 - S_4$ and Figure S_3). These were based on the data from combined cycles. Additional PMF results by cycle (season), are also presented in supplemental materials (Tables $S_5 - S_6$ and Figures $S_4 - S_7$).

The interpretation and identification of the model factors to determine the emission sources of $PM_{2.5}$ was done using comparisons of factor loadings in the profiles of pollutant species. Generally, the chemical pollutants measured in air originate from specific sources and thus can be used as markers for those sources.

The first factor explaining the largest proportion (30.1%) of $PM_{2.5}$ was identified as vehicular/automobile emissions due to their high contributions to the profiles of Mg, Al, K, Ca, Ti, Cr, Mn, Fe, Ni, Cu, Zn, Ga, Rb, Sr, Ce, and BC. The TEs and other pollutants emitted from automobiles may come from combustion of fuel (gasoline or diesel), the engine oils (Cu, Zn, Ni), tires or brake pads (Pant and Harrison, 2013). Some of the major and common elements from car tires include Fe, Mn, Ca, Mg, Na, K, Al, Zn and Sb. A preliminary examination report on TEs in tires, brake pads and road bitumen in New Zealand (Jennifer and Paul, 2003) reported heavy metals including Pb and Cd in car tires. The same study identified several elements in brake pads that are classified as major TEs (Ca, Mg, Na, K, Al, Fe, Mn, Ti), priority pollutants (Cu, Zn, Ni, Cr, Pb), non-essential TEs (Ce, Sr, Rb, Ga) and metal sulfides (Cu_2S, PbS, Sb_2S_3). While the majority of these TEs were classified as earth-crust derived in the EF analysis, some proportion originated from vehicular emissions as shown by the PMF analysis. Makkah City has heavy automobile traffic, which is reflected in the contribution of vehicular emissions to the overall $PM_{2.5}$.

The second factor was identified as industrial mixed dust and explained 28.9% of the total variation in $PM_{2.5}$, due to the contributions to the profiles of Na, Mg, Al, Si, S, Cl, K, Ca, Ti, Cr, Mn, Fe, Ni, Cu, Zn, Br, Rb, Sr, Er, Lu and BC. Central Makkah City is not industrialized. However, dust from industries within the region (such as oil refineries, desalination plants, steel processing, cement and concrete, chemical industries), contributed significant proportions to the overall $PM_{2.5}$ observed in this study. Notably, during the study there was major infrastructural development occurring in Makkah involving the extension of grand mosque and first ring road restructuring. This involved extensive construction and demolition activities. Thus, the elements associated with cement and concrete industries, such as Na, Mg, Al, Si, S, Cl, K, Ca, Ti, Cr, Mn, Fe, Zn, and Sr (Zhang et al., 2018; Vollpracht and Brameshuber, 2016), were highly enriched in the air. Also, the backward-in-time wind trajectories Also, the backward-in-time wind trajectories (Figures $S_8 - S_{11}$) indicated that the regional transport of industrial dust may be a major contributor to air pollution in Makkah. Na, Cl, K and Mg may also be attributed to regional transport of marine aerosols from Red Sea. However, Sea Spray was not a clearly resolved factor in our PMF model. Future studies with more chemical species analyzed from $PM_{2.5}$, may be able to resolve this factor with PMF analysis.

The third factor was soil/earth-crust, which explained 24.7% of

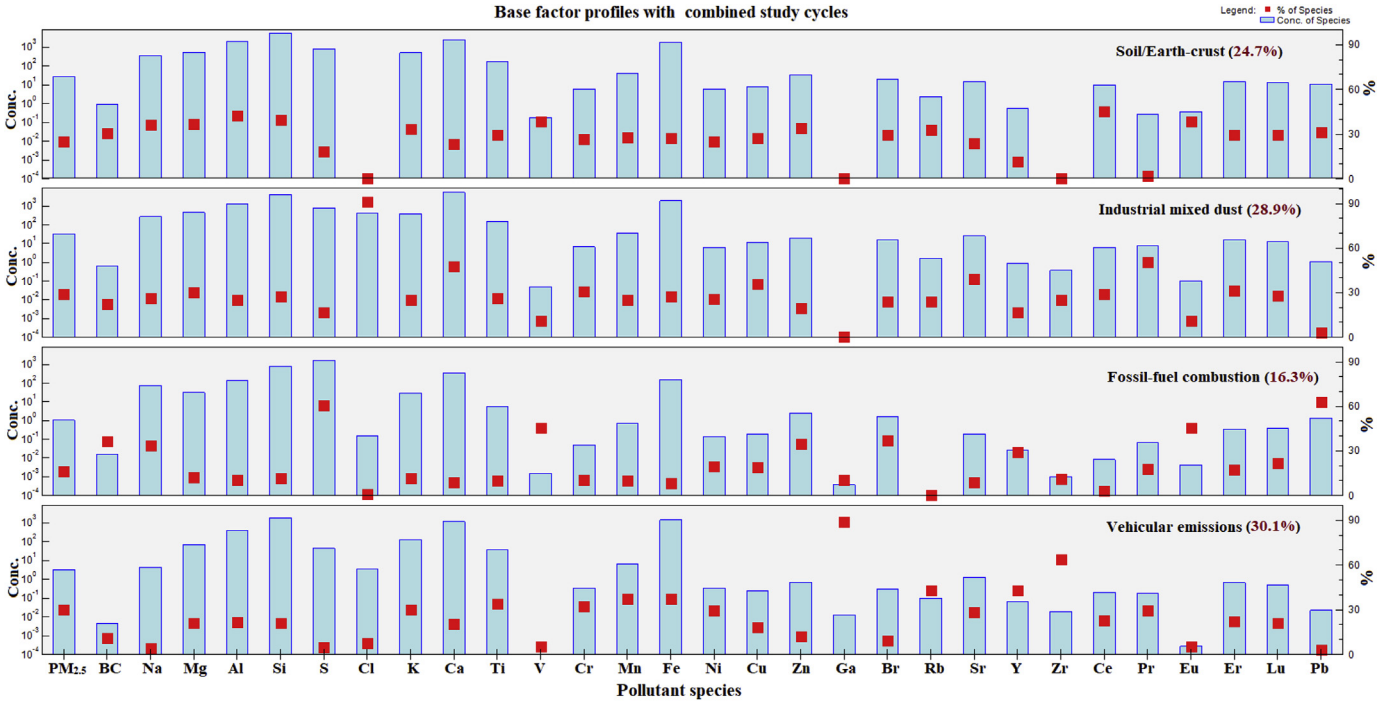

Fig. 6. Base factor profiles and the relative factor contributions to the overall $PM_{2.5}$ – Makkah cycles_1 – 4 combined.

the overall $PM_{2.5}$. This factor contributed significantly to the profiles of Na, Mg, Al, Si, K, Ti, Cr, Mn, Fe, Ca, and Pb. The arid climate, which is characterized with occasional sand storms, already serves as a significant source of resuspended sand/dust. Combined with the ongoing construction work, plus heavy automobile traffic during Makkah dust re-suspension significantly contributed to the elevated $PM_{2.5}$ in this study. The crustal elements (Si, Ca, Fe, Al, K, Mg) consistently had the highest concentrations across all the 4 cycles (Table 1). Some rare earth elements (Lu, Er, Rb, Ce) were also observed in this factor. The soil enrichment of these elements may be linked to contamination from anthropogenic activities mostly related to regional industrial and local vehicular emissions.

The fourth factor (fossil-fuels/oil combustion) explained 16.3% of the total variation in $PM_{2.5}$. This factor contributed significantly to the profiles of S, Pb, V, Zn, Br, Cu, Ni, Y, Lu, Na and BC. Black carbon is emitted as a by-product of incomplete combustion processes. S is emitted as SO_2, and V exists naturally as an impurity in the fossil-fuel deposits. Lu isotopes are used as catalysts in the petrochemical industries and Br compounds have several applications as earlier noted.

3.6. Backward-in-time trajectories

Plots of backward-in-time wind trajectories were used to determine the influence of local and regional sources to the $PM_{2.5}$ measured in Makkah. Figures S_8 to S_{11} show the wind trajectories 72-h prior to sampling for the 2 days with the highest and 2 days with lowest $PM_{2.5}$ measurements per sampling cycle (season) in Makkah.

Across all the four sampling cycles, the days with the lowest $PM_{2.5}$ levels had wind trajectories blowing over the Red Sea into the sampling sites. The air above the sea has significantly lower PM levels, which introduces a dilution effect to the ambient PM concentrations. In contrast, for those days with the highest $PM_{2.5}$ levels, the wind trajectories were passing over heavily industrialized areas and other inland areas. The ambient $PM_{2.5}$ levels over these areas were much higher than those over the Red Sea, which significantly supplemented the local emissions in Makkah. Also, severe weather with dust storms resulted in elevated $PM_{2.5}$. The two days in cycle_1 (April 11 to 12, 2014) with the highest $PM_{2.5}$ levels were days with wide-spread sand-storms that significantly spiked the ambient $PM_{2.5}$ levels.

Backward-in-time wind trajectories can also be used to assess the regional distribution of air pollutants by simply tracing the path of the wind current. The chemical constituents of $PM_{2.5}$ vary significantly based on the path of the wind currents. For example, elevated levels of crustal TEs (Al, Mg, Si, Ca, Fe, etc.) were measured when the wind trajectories blew across the inland areas, and higher levels of anthropogenic TEs (S, V, Cr, Lu, Pb, Ce, Br, etc.) were characteristic of trajectories passing over heavily industrialized cities.

4. Summary and conclusions

Particulate air pollution remains a significant issue in Makkah. There were significant temporal variabilities in PM levels with average $PM_{2.5}$ per cycle far exceeding both the 24-h PME ($35\ \mu g\ m^{-3}$) and WHO ($25\ \mu g\ m^{-3}$) air quality guidelines. Computations of AQI indicated an unhealthy to hazardous air quality index during most of the study period, further highlighting the poor state of ambient air quality in Makkah.

Anthropogenic contributions to air pollution in Makkah were primarily related to construction, local vehicular, and regional industrial emissions. More than 75% of the total $PM_{2.5}$ emissions in this study were attributed to anthropogenic sources (vehicular emissions, fossil-fuels/oil combustion, and industrial mixed dust) as shown by the PMF analysis. Also, the backward-in-time wind trajectories showed that long-distance/regional transport of $PM_{2.5}$ may be a major source of air pollution in Makkah.

A minor limitation of this study relates to the number of pollutant species analyzed from $PM_{2.5}$. This may have influenced the PMF resolution on the number of factors. However, the overall results from this study are consistent with findings from previous studies and further document the serious problem of air pollution in urban areas of Saudi Arabia. While air pollution from sand storms cannot be easily controlled, most air pollution was related to anthropogenic activities. Establishing and enforcing regulations on the anthropogenic sources of air pollution is essential for the protection of the health of the public in Saudi Arabia and the rest of the Middle East region. There is a need for regional rather than just local action, given the evidence for long-distance/regional transport of air pollutants.

Conflicts of interest

The authors declare no competing interests.

Acknowledgements

This study was supported by a grant from King Abdulaziz University, Jeddah, Saudi Arabia. Authors acknowledge the Civil Defense of the Makkah region, as well as the Aburizaiza and Ramadani families, for their support in the sampling campaign. The authors also acknowledge assistance from the NOAA Air Resources Laboratory (ARL) for the provision of HYSPLIT transport and dispersion model (http://www.ready.noaa.gov) used in this study. We also extend our thanks to Dr. Lung C. Chen, New York University School of Medicine, for his excellent support in analyzing trace metals and Dr. Kim McClive-Reed for editing the manuscript.

Appendix A. Supplementary data

Supplementary data to this article can be found online at https://doi.org/10.1016/j.envpol.2018.09.086.

References

Ahmed, T., Dutkiewicz, V.A., Shareef, A., Tuncel, G., Tuncel, S., Husain, L., 2009. Measurement of black carbon (BC) by an optical method and a thermal-optical method: intercomparison for four sites. Atmos. Environ. 43 (40), 6305–6311.
Akyuz, M., Cabuk, H., 2009. Meteorological variations of $PM_{2.5}/PM_{10}$ concentrations and particle-associated polycyclic aromatic hydrocarbons in the atmospheric environment of Zonguldak, Turkey. J. Hazard Mater. 170 (1), 13–21.
Al-Jeelani, H.A., 2009a. 'Air quality assessment at Al-Taneem area in the holy makkah city, Saudi Arabia. Environ. Monit. Assess. 156 (1–4), 211–222.
Al-Jeelani, H.A., 2009b. Evaluation of air quality in the holy makkah during Hajj season 1425 H. J. Appl. Sci. Res. 5 (1), 115–121.
Alharbi, B., Shareef, M.M., Husain, T., 2015. Study of chemical characteristics of particulate matter concentrations in Riyadh, Saudi Arabia. Atmospheric Pollution Research 6 (1), 88–98.
Amarsaikhan, D., Battsengel, V., Nergui, B., Ganzorig, M., Bolor, G., 2014. A study on air pollution in ulaanbaatar city, Mongolia. J. Geosci. Environ. Protect. 2 (02), 123.
Anderson, H., Bremner, S., Atkinson, R., Harrison, R., Walters, S., 2001. Particulate matter and daily mortality and hospital admissions in the west midlands conurbation of the United Kingdom: associations with fine and coarse particles, black smoke and sulphate. Occup. Environ. Med. 58 (8), 504–510.
Aprile, F.M., Bouvy, M., 2008. Distribution and enrichment of heavy metals in sediments at the tapacurá river basin, northeastern Brazil. Braz. J. Aquat. Sci. Technol. 12 (1), 1–8.
Begum, B.A., Hossain, A., Nahar, N., Markwitz, A., Hopke, P.K., 2012. Organic and black carbon in $PM_{2.5}$ at an urban site at Dhaka, Bangladesh. Aerosol and Air Quality Research 12 (6), 1062–1072.
Bell, M.L., Dominici, F., Ebisu, K., Zeger, S.L., Samet, J.M., 2007. Spatial and temporal variation in $PM_{2.5}$ chemical composition in the United States for health effects studies. Environ. Health Perspect. 115 (7), 989–995.
Bleiwas, D.I., 2013. Potential for Recovery of Cerium Contained in Automotive

Catalytic Converters. U.S. Department of the Interior, Reston, Virginia, p. 10. U.S. Geological Survey Open-File Report 2013–1037.
Brown, K.W., Bouhamra, W., Lamoureux, D.P., Evans, J.S., Koutrakis, P., 2008. Characterization of particulate matter for three sites in Kuwait. J. Air Waste Manag. Assoc. 58 (8), 994–1003.
Buhrke, V.E., Jenkins, R., Smith, D.K., 1998. Practical Guide for the Preparation of Specimens for X-ray Fluorescence and X-ray Diffraction Analysis.
Degobbi, C., Lopes, F.D.T.Q.S., Carvalho-Oliveira, R., Muñoz, J.E., Saldiva, P.H.N., 2011. Correlation of fungi and endotoxin with $PM_{2.5}$ and meteorological parameters in atmosphere of Sao Paulo, Brazil. Atmos. Environ. 45 (13), 2277–2283.
Fabretti, J.-F., Sauret, N., Gal, J.-F., Maria, P.-C., Schärer, U., 2009. Elemental characterization and source identification of $PM_{2.5}$ using Positive Matrix Factorization: the Malraux road tunnel, Nice, France. Atmos. Res. 94 (2), 320–329.
Habeebullah, T.M., 2013. 'An analysis of air pollution in makkah - a view point of source identification. Environment Asia 6 (2), 11.
Hamad, S.H., Schauer, J.J., Heo, J., Kadhim, A.K.H., 2015. Source apportionment of $PM_{2.5}$ carbonaceous aerosol in Baghdad, Iraq. Atmos. Res. 156, 80–90.
Hopke, P.K., 2000. A Guide to Positive Matrix Factorization (PMF).
Hueglin, C., Gehrig, R., Baltensperger, U., Gysel, M., Monn, C., Vonmont, H., 2005. Chemical characterisation of $PM_{2.5}$, PM_{10} and coarse particles at urban, near-city and rural sites in Switzerland. Atmos. Environ. 39 (4), 637–651.
Jennifer, G., Paul, K., 2003. Preliminary Examination of trace Elements in tyres, brake Pads and road Bitumen in New Zealand: ministry of transport, New Zealand. Available at: http://www.transport.govt.nz/assets/Import/Documents/stormwater-inorganic3.pdf. (Accessed 25 March 2018).
Kermani, M., Arfaeinia, H., Nabizadeh, R., Alimohammadi, M., Aalamolhoda, A., 2015. Levels of $PM_{2.5}$ - associated heavy metals in the ambient air of Sina hospital district, Tehran, Iran. J. Air pollution & Health 1 (1), 1–6.
Khan, M.F., Shirasuna, Y., Hirano, K., Masunaga, S., 2010. Characterization of $PM_{2.5}$, $PM_{2.5-10}$ and PM_{10} in ambient air, Yokohama, Japan. Atmos. Res. 96 (1), 159–172.
Khodeir, M., Shamy, M., Alghamdi, M., Zhong, M., Sun, H., Costa, M., Chen, L.-C., Maciejczyk, P., 2012. Source apportionment and elemental composition of $PM_{2.5}$ and PM_{10} in Jeddah city, Saudi Arabia. Atmos. Pollution Res. 3 (3), 331–340.
Kłos, A., Rajfur, M., Wacławek, M., Wacławek, M., 2011. Application of enrichment factor (EF) to the interpretation of results from the biomonitoring studies. Ecol. Chem. Eng. 18 (2), 171–183.
Korzhova, E.N., Kuznetsova, O.V., Smagunova, A.N., Stavitskaya, M.V., 2011. Determination of inorganic pollutants in atmospheric aerosols. J. Anal. Chem. 66 (3), 222–240.
Kulshrestha, A., Satsangi, P.G., Masih, J., Taneja, A., 2009. Metal concentration of $PM_{2.5}$ and PM_{10} particles and seasonal variations in urban and rural environment of Agra, India. Sci. Total Environ. 407 (24), 6196–6204.
Margui, E., Van Grieken, R., 2013. X-Ray Fluorescence Spectrometry and Related Techniques. Momentum Press, LLC, New York.
Munir, S., Habeebullah, T.M., Seroji, A.R., Gabr, S.S., Mohammed, A.M.F., Morsy, E.A., 2013. Modeling particulate matter concentrations in makkah, applying a statistical modeling approach. Aero. Air Qual. Res. 13 (3), 901–910.
Nakhle, M.M., Farah, W., Ziade, N., Abboud, M., Coussa-Koniski, M.L., Annesi-Maesano, I., 2015. Beirut air pollution and health effects - BAPHE study protocol and objectives. Multidiscip. Respir. Med. 10 (1), 21.
Nasrallah, M.M., Seroji, A.R., 2008. Particulates in the atmosphere of makkah and mina valley during ramadhan and Hajj season of 1424 and 1425 H (2004 – 2005). Arab Gulf J. Sci. Res. 26, 199–206.
Nayebare, S.R., 2016. Fine Particulate Air Pollution in Saudi Arabia—Implications for Cardiopulmonary Morbidity. Ph.D., State University of New York at Albany.
Nayebare, S.R., Aburizaiza, O.S., Khwaja, H.A., Siddique, A., Hussain, M.M., Zeb, J., Khatib, F., Carpenter, D.O., Blake, D.R., 2016. Chemical characterization and source apportionment of $PM_{2.5}$ in Rabigh, Saudi Arabia. Aero. Air Qual. Res. 16 (12), 3114–3129.
Ozturk, F., Zararsiz, A., Kirmaz, R., Tuncel, G., 2011. An approach to measure trace elements in particles collected on fiber filters using EDXRF. Talanta 83 (3), 823–831.
Pant, P., Harrison, R.M., 2013. Estimation of the contribution of road traffic emissions to particulate matter concentrations from field measurements: a review. Atmos. Environ. 77 (1), 78–97. https://doi.org/10.1016/j.atmosenv.2013.04.028.
Pateraki, S., Assimakopoulos, V.D., Maggos, T., Fameli, K.M., Kotroni, V., Vasilakos, C., 2013. Particulate matter pollution over a Mediterranean urban area. Sci. Total Environ. 463–464, 508–524.
Rattigan, O.V., Civerolo, K., Doraiswamy, P., Felton, H.D., Hopke, P.K., 2013. Long term black carbon measurements at two urban locations in New York. Aerosol and Air Quality Research 13 (4), 1181–1196.
Reimann, C., Caritat, P. d., 2000. Intrinsic flaws of element enrichment factors (EFs) in environmental geochemistry. Environ. Sci. Technol. 34 (24), 5084–5091.
RSC, 2016. Royal society of chemistry (RSC): uses and properties of Lutetium (Lu). Available at: http://www.rsc.org/periodic-table/element/71/lutetium. (Accessed 6 June 2016).
SADP, 2014. Saudi Arabia Demographic Profile 2014. Available at: http://www.indexmundi.com/saudi_arabia/demographics_profile.html. (Accessed 5 April 2016).
Shaltout, A.A., Boman, J., Al-Malawi, D.A.R., Shehadeh, Z.F., 2013. Elemental composition of $PM_{2.5}$ particles sampled in industrial and residential areas of taif, Saudi Arabia. Aerosol and Air Quality Research 13 (4), 1356–1364.
Sillanpää, M., Frey, A., Hillamo, R., Pennanen, A.S., Salonen, R.O., 2005. Organic, elemental and inorganic carbon in particulate matter of six urban environments in Europe. Atmos. Chem. Phys. 5 (11), 2869–2879.
Simpson, I.J., Aburizaiza, O.S., Siddique, A., Barletta, B., Blake, N.J., Gartner, A., Khwaja, H., Meinardi, S., Zeb, J., Blake, D.R., 2014. Air quality in Mecca and surrounding holy places in Saudi Arabia during Hajj: initial survey'. Environ. Sci. Technol. 48 (15), 8529–8537.
Sofowote, U.M., McCarry, B.E., Marvin, C.H., 2008. Source apportionment of PAH in Hamilton harbour suspended sediments: comparison of two factor analysis methods. Environ. Sci. Technol. 42 (16), 6007–6014.
Steinbach, C., 2011. Cerium Dioxide (CeO2) - Overview nanopartikel.info (2011-02-02). Available at: http://nanopartikel.info/en/nanoinfo/materials/cerium-dioxide. (Accessed 6 June 2016).
Taylor, S.R., 1964. Abundance of chemical elements in the continental crust: a new table. Geochem. Cosmochim. Acta 28 (8), 1273–1285.
Trovarelli, A., 2002. Catalysis by Ceria and Related Materials. Imperial College Press, pp. 6–11.
Vollpracht, A., Brameshuber, W., 2016. Binding and leaching of trace elements in Portland cement pastes. Cement Concr. Res. 79, 76–92.
Wang, Y., Hopke, P.K., Rattigan, O.V., Chalupa, D.C., Utell, M.J., 2012. Multiple-year black carbon measurements and source apportionment using Delta-C in Rochester, New York. J. Air Waste Manag. Assoc. 62 (8), 880–887.
Wang, Y., Hopke, P.K., Rattigan, O.V., Xia, X., Chalupa, D.C., Utell, M.J., 2011. Characterization of residential wood combustion particles using the two-wavelength aethalometer. Environ. Sci. Technol. 45 (17), 7387–7393.
Xu, H.M., Cao, J.J., Ho, K.F., Ding, H., Han, Y.M., Wang, G.H., Chow, J.C., Watson, J.G., Khol, S.D., Qiang, J., Li, W.T., 2012. Lead concentrations in fine particulate matter after the phasing out of leaded gasoline in Xi'an, China. Atmos. Environ. 46 (0), 217–224.
Yatkin, S., Gerboles, M., Borowiak, A., 2012. Evaluation of standardless EDXRF analysis for the determination of elements on PM_{10} loaded filters. Atmos. Environ. 54 (0), 568–582.
Yatkin, S., Bayram, A., 2008. Source apportionment of PM_{10} and $PM_{2.5}$ using positive matrix factorization and chemical mass balance in Izmir, Turkey. Sci. Total Environ. 390 (1), 109–123.
Zeng, J., He, Q., Zhou, H., Sun, X., Zhang, J., 2012. Recovery of cerium(III) from aqueous solutions by complexation—ultrafiltration process. Asia Pac. J. Chem. Eng. 7 (6), 940–947.
Zhang, M., Yang, C., Zhao, M., Yu, L., Yang, K., Zhu, X., Jiang, X., 2018. Immobilization of Cr(VI) by hydrated Portland cement pastes with and without calcium sulfate. J. Hazard Mater. 342, 242–251.
Zhao, X., Zhang, X., Xu, X., Xu, J., Meng, W., Pu, W., 2009. Seasonal and diurnal variations of ambient $PM_{2.5}$ concentration in urban and rural environments in Beijing. Atmos. Environ. 43 (18), 2893–2900.